Removal of synthetic and industrial effluent color by photocatalytic process

Bruna de Paula Soares, Leticia Rosa Climaco, Lariana Negrão Beraldo de Almeida and Giane Gonçalves Lenzi

ABSTRACT

The present work aimed at evaluating the photocatalytic process as an alternative for color removal from a synthetic solution (methylene blue dye) and of a sample of textile effluent, obtained from the various stages of the process, mainly dyeing. The parameters were evaluated using titanium dioxide (anatase, rutile, commercial and synthetized by the sol-gel method) in order to determine their structural influence in the discoloration of the samples. A synthetic methylene blue dye solution and a real effluent (Brazilian textile industry) were treated. The photocatalytic degradation was carried out over three hours in a batch reactor, under constant agitation, aeration, radiation and temperature. It was observed that the characteristics of each catalyst directly influence the photocatalytic activity. As a result, for the variables used in this work, the photocatalyst TiO_2 anatase phase with a concentration of 1 kg/m^3 was the most efficient condition, presenting full color removal for the methylene blue and 71% for the sifted textile effluent.

Key words | color removal, effluent treatment, heterogeneous photocatalysis process, textile industry, titanium dioxide

Bruna de Paula Soares (corresponding author)
Leticia Rosa Climaco
Federal Technological University of Paraná,
Monteiro Lobato Avenue, Zip code: 84016-210,
Ponta Grossa, Paraná,
Brazil
E-mail: *brunasoares494@gmail.com*

Lariana Negrão Beraldo de Almeida
State University of Maringá,
Colombo Avenue, 5790, Zip code: 87020-900,
Maringá, Paraná,
Brazil

Giane Gonçalves Lenzi
Federal Technological University of Paraná,
Monteiro Lobato Avenue, km 04, Zip code: 84016-210, Ponta Grossa, Paraná,
Brazil

INTRODUCTION

Currently, in the textile industries, many processes are carried out from the fibers to the final product (Ahmad & Hameed 2009). In one of the stages of the process, dyes are used to give permanent color to other substances, mainly applied to color fiber and textile fabrics (Lenzi *et al.* 2015). In particular, in the jeans washing process, a high amount of water is used and consequently a large amount of effluent is generated. These effluents are composed of substances of slow biodegradability, high biochemical oxygen demand (BOD), high presence of dissolved salts and synthetic dyes, with high detergent content and toxic substances, which make it difficult to treat these effluents (Sales Solano *et al.* 2013).

Methylene blue (MB), a typical textile dye (Xiong *et al.* 2011), has its structure and characteristics shown in Table 1.

Due to the great environmental impact, many researchers have sought alternatives for the degradation of dyes, one of these choices having been heterogeneous photocatalysis, since this method can degrade complex compounds such as the structure of the dyes into simpler and less toxic compounds (Hathaisamit *et al.* 2012; Dhanya & Aparna 2016; Landi *et al.* 2017). Advanced oxidative processes (AOP) are based on the creation of strong oxidative agents, such as the hydroxyl radical (OH^-), which can degrade and mineralize chemical compounds (Tokode *et al.* 2017). Among these processes, there is heterogeneous photocatalysis, in which the use of photocatalytic semiconductors for reaction occurs. Among the semiconductors used, titanium dioxide (TiO_2) is widely used as a catalyst. This is due to its attractive properties, such as non-toxicity, photochemical stability and low cost (Fujishima *et al.* 2000; Carp *et al.* 2004; Han *et al.* 2009). Some investigations use TiO_2 for the degradation of several compounds, such as in the discoloration of the reactive blue 5 g dye (Souza *et al.* 2011), in the reduction of mercury (II) (Lenzi *et al.* 2011), in the degradation of *Escherichia coli* bacteria (Helali *et al.* 2013; Miranda *et al.* 2016) among others.

Thus, the objective of this work was to establish a comparison among different forms of TiO_2 catalysts: sol-gel preparation, rutile and anatase forms and commercial. In addition, after optimization of the process using a synthetic effluent (methylene blue solution), the optimum conditions were applied in a real effluent from a Brazilian textile industry.

doi: 10.2166/wst.2018.264

Table 1 | Structure and characteristics of methylene blue

Structure	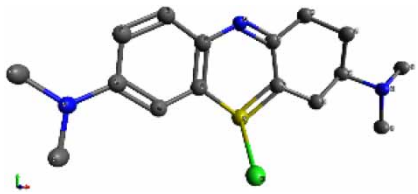
Solubility in water (kg/m³) (20 °C)	20
M_w (g/mol)	0.3738
λ_{max} (nm)	660

METHODS

Catalysts

The tests were performed using different forms of titanium dioxide (TiO_2), shown in Table 2.

Synthetic solution and real effluent

The methylene blue solution with a concentration of 0.02 kg/m³ was used as a validation model to optimize the parameters. A sample of sifted textile effluent (effluent pretreatment made in the textile industry) and a sample of textile effluent untreated (without any chemical and physical pretreatment) were used, from an industrial laundry located in the city of Curitiba in Brazil.

Optimization of parameters

The four titanium dioxide forms mentioned above were tested in the photocatalytic process using the methylene blue solution as the validation model. For the best of the results among the catalysts, different concentrations of catalyst in the solution (0.5, 1 and 2 kg/m³) were tested in the sifted textile effluent solution. After adjusting these parameters, the photocatalytic process was repeated under the best conditions for the untreated textile effluent.

Characterization

Photoacoustic spectroscopy (PAS)

The photoacoustic spectroscopy measurements in the UV–VIS spectral regions were performed using a laboratory-made experimental setup. We obtained the monochromatic light through a 1000-Watt xenon arc lamp (Oriel Corporation 68820) and a monochromator model 77250, also by Oriel Instruments. We modulated the light beam using a mechanical chopper – Stanford Research Systems SR540. A lab-made photoacoustic cell was designed to have a very low volume – made of aluminum block, machined to hold samples with dimensions up to 5 mm diameter and 1 mm thickness, which allows light to enter through a high transparency quartz window of 6 mm diameter and 2 mm thickness. The size of the microphone chamber was 15 mm; it was connected to the sample holder room through a 1-mm diameter duct. The capacitive microphone used was the 12-mm diameter Bruel & Kjaer model 2639 – very sensitive, presenting a gain of 50 mV/Pa, with a flat frequency response between 1 Hz and 10 kHz. A lock-in amplifier by EG & G Instruments, model 5110, was used. All the photoacoustic spectra were obtained at a 20 Hz modulation frequency and recorded between 220 and 720 nm. Data were acquired using a personal computer, and the PAS spectra were normalized with respect to the carbon black signal.

The band gap energies were established through Equation (1):

$$\lambda = \frac{hc}{E_{gap}} = \frac{1240}{E_{gap}} \quad (1)$$

Table 2 | Catalyst specifications

Catalyst	Preparation	Supplied	Purity (%)
TiO_2 Commercial	Non-calcined	Perquim	[a]
TiO_2 Rutile form	Calcined at 623.15 K	Sigma-Aldrich	99.9
TiO_2 Anatase form	Calcined at 623.15 K	Sigma-Aldrich	99.9
TiO_2 Sol-gel	Chemical mixing method	Synthetized[b]	–

[a]Not indicated.

[b]TiO_2 sol-gel (chemical mixing method, more details (Lenzi *et al.* 2011)) previously prepared by adding titanium isopropoxide 98% P.A. (supplied by Across Organics) in an inert argon atmosphere and isopropanol 99.5% P.A. (supplied by Fmaia) previously acidified with HNO_3 65% P.A (supplied by Fmaia), molar ratio HNO/Ti = 0.15 (Oropeza *et al.* 2010). The calcination was carried out in gradual heating to 623.15 K in a muffle furnace.

where E_{gap} is the band gap energy in eV units. The direct method was applied to obtain the values, i.e., $m = 2$.

Textural properties

Porous properties such as specific surface area, mean pore diameter, and pore volume were established using a Quantachrome analyzer – model Nova-1200 with N2 adsorption at 77 K. Both calcined and non-calcined samples were submitted to these analyses. The samples had been previously submitted to a thermal treatment at 573 K, under 2-hour vacuum to eliminate any existing water within the pores of the solids.

X-ray diffraction

The samples were measured through a Rigaku-Denki Diffractometer with Cu-Kα radiation ($\lambda = 1.5406$ Å) at 140 V voltage and 40 mA current; subsequently, the patterns obtained were compared with the diffraction dataset cards from the Joint Committee of Powders Diffraction Standards (JCPDS).

Characterization of the real effluent

The industrial textile effluent was quantitatively characterized (Table 3). These parameters were determined using the Pastel UV – Secomam spectrophotometer in triplicates.

Photocatalytic tests

The reaction mixture was stored in a reactor of Pyrex glass. We conducted the tests over 3 hours; opened to the air and to an oxygen stream and bubbled into suspension. A 250 W medium pressure mercury lamp, which had its original protective bulb removed, was used for irradiation. In order to maintain room temperature, we surrounded the vessel with a jacket in which cold water flows. The reactor contained a magnetic stirrer to ensure the homogeneity of the reaction mixture. At regular intervals, an aliquot of the suspension was withdrawn and centrifuged to promote the separation of the catalyst from the solution, providing a better visualization of the coloration. The discoloration of the solutions as a function of time was established through a Shimadzu UV-1203 UV/Vis spectrophotometer (= 670 *nm*). The adsorption tests were performed applying the same procedure as the photocatalytic test, but without the presence of light. The photolysis test experiments were conducted using no catalysts and following the same procedure as for the photocatalytic tests.

RESULTS AND DISCUSSION

The results obtained by photoacoustic spectroscopy (PAS) (band gap) for commercial TiO_2, anatase, rutile and sol-gel, calcined at 623.15 K, are presented in Figure 1(a)–1(d) respectively and described in Table 4.

The band gap values were obtained in the range of 3.05–3.19 eV. The growing sequence was rutile < sol-gel < anatase < commercial as shown in Table 4. These gaps indicate quite positive potentials, in the range of +2.0 to +3.5 V, depending on the semiconductor (Vohra & Tanaka 2003).

Commercial TiO_2 presented a high band gap value (3.19 eV), which is in agreement with the literature (Vamathevan *et al.* 2001). In the anatase form, the obtained band gap value was 3.14 eV ($\lambda = 395$ nm), and this form of TiO_2 is indicated in the literature as the most photoactive in relation to other forms of TiO_2 (Gupta & Tripathi 2011). The sol-gel catalyst obtained a band gap of 3.12 eV ($\lambda =$ 397 nm), showing that the synthesis of TiO_2 by the sol-gel method resulted in a decrease of the band gap, compared to commercial TiO_2 and the anatase form. On the other hand, the TiO_2 catalyst in the rutile form presented a band

Table 3 | Effluent characterization

Effluent	Characterization	Methodology
Sieved and untreated	Chemical oxygen demand (COD) (evaluates the amount of dissolved oxygen (DO) consumed in an acid medium that leads to the organic matter degradation). Biochemical oxygen demand (BOD) (the oxygen amount required to oxidize biodegradable organic matter). Total dissolved solids (TDS) (evaluates the total weight of mineral constituents present in the water).	The samples (1 mL) were homogenized and inserted into the quartz cell. The response of the parameters is in $mg{\cdot}L^{-1}$.

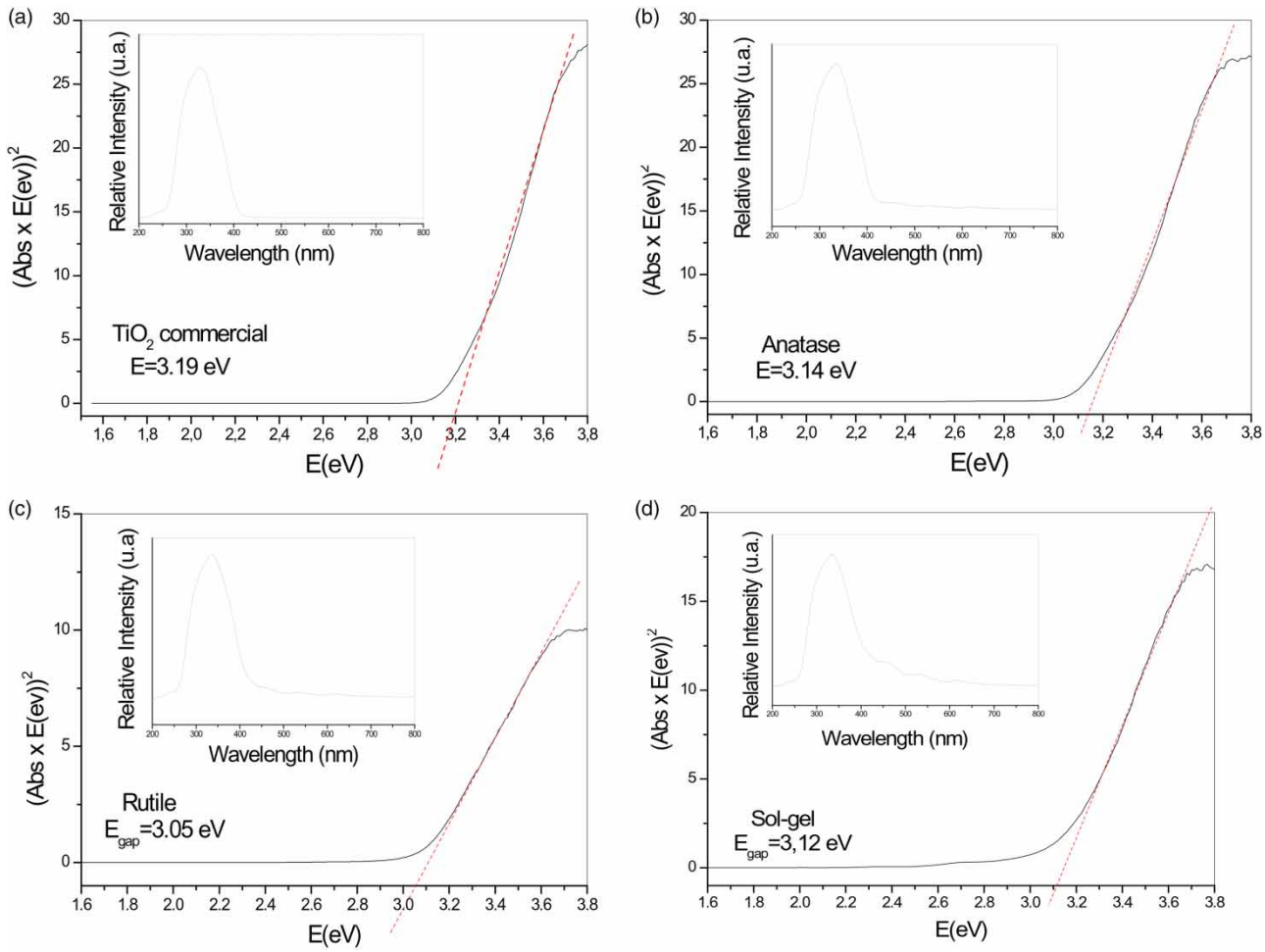

Figure 1 | Band gap results for TiO_2: (a) commercial; (b) anatase; (c) rutile; and (d) sol-gel.

gap of 3.05 eV ($\lambda = 406$ nm), presenting the lowest value among the catalysts studied.

With the smallest band gap of the commercial catalyst, it was expected that with the smaller distance between the conduction band and valence band, it could facilitate the electronic excitation and improve the efficiency of the catalyst. However, it should be taken into account that, besides the band gap, a large number of variables affect the overall efficiency of the photocatalytic process in the aqueous phase. Among these variables are: crystalline phase, photocatalyst doping level, particle size uniformity, active surface area, aggregate porosity, incident light radiance and temperature.

Table 4 | Band gap results for semiconductors

Catalyst TiO_2	Band gap (eV)	Absorption threshold (nm)
Commercial	3.05	406
Anatase	3.12	397
Sol-gel	3.14	395
Rutile	3.19	389

Figure 2 shows the X-ray diffraction (XRD) patterns of TiO_2 rutile, anatase, commercial and prepared by the sol-gel method forms. For the TiO_2 in anatase form only crystalline anatase phase were found: $2\theta = 25.32°$; 36.95°; 37.81°; 38.58°; 48.04°; 53.9°; 55.07°; 62.7° e 68.77°. For the rutile phase: $2\theta = 27.49°$; 36.10°; 39.22°; 41.27°; 44.15°; 54.30°; 56.66°, these data are in accordance with those described in the literature (Cai *et al.* 2013). For the commercial TiO_2 were found: $2\theta = 27.49°$; 36.10°; 39.13°; 41.27°; 44.21°; 54.30°. The sol-gel catalyst has an amorphous structure.

The results obtained for the textural properties are presented in Table 5. It can be seen that the largest specific surface area was obtained for the catalyst prepared by the sol-gel method. As described in the literature (Lenzi *et al.*

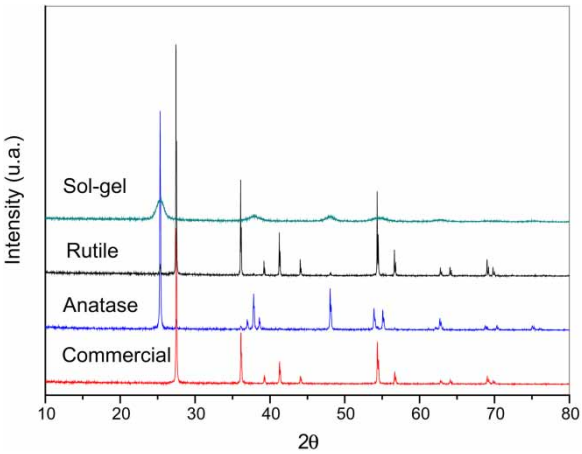

Figure 2 | XRD spectra of the TiO_2.

2008), this method has the characteristic of obtaining materials with high surface areas. The surface areas of commercial TiO_2 and anatase were close (12.74 and 10.42 m^2/g, respectively); in the literature, values are found in the range of 7–9 m^2/g (Lenzi *et al.* 2011). For the rutile form, a surface area of 2.70 m^2/g was obtained.

Photocatalytic tests

Synthetic effluent: for the experimental tests with the methylene blue solution, the initial concentration of the solution was 0.02 kg/m^3. The percentages of color removal using TiO_2 rutile and anatase forms are described respectively in Figure 3(a) and 3(b) and for the other catalysts in the sequence. The values obtained in the photocatalytic test with the synthetic solution of methylene blue dye can be described by the first-order kinetic model $ln(C_0/C) = kt$, where C_0 is the initial concentration and C the concentration at any time t and k is the reaction rates constant. From this equation, a graph of $ln(C_0/C)$ was plotted as a function of time t and the angular coefficient is the term k (detail of Figure 3(a) and 3(b)), which allowed to determine the reaction rates constant experimentally (Souza *et al.* 2011).

Table 5 | Summarizes the surface textural properties catalysts TiO_2

Catalysts	Specific surface area, S_o (m^2/g)	Pore volume (cm^3/g)	Average pore diameter (Å)
TiO_2 commercial	13	0.0090	29.89
TiO_2 anatase	10	0.0131	25.16
TiO_2 sol-gel	154	0.2603	33.80
TiO_2 rutile	3	0.0042	31.13

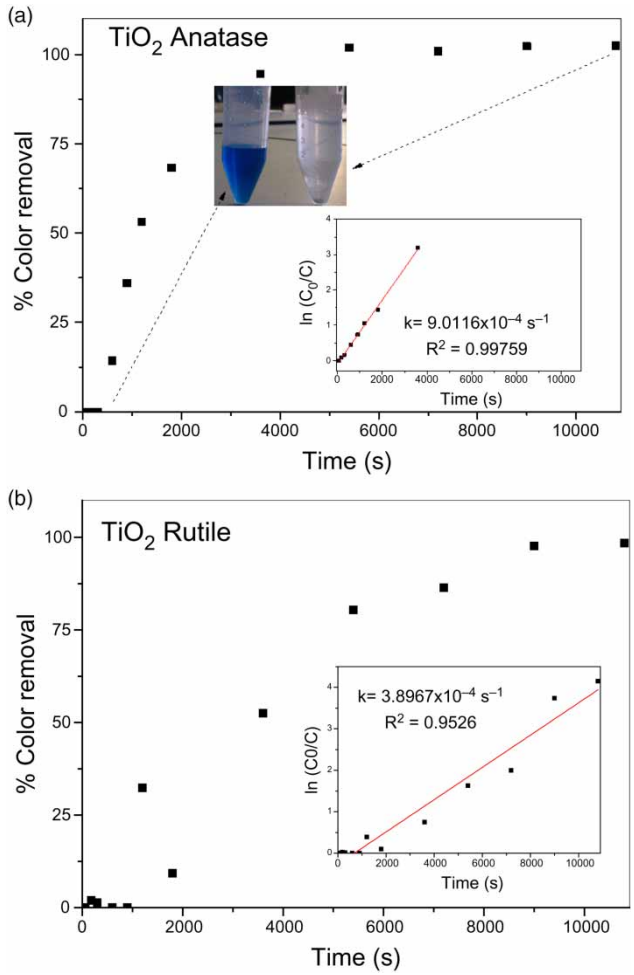

Figure 3 | Photocatalytic test with synthetic solution: TiO_2 (a) anatase; (b) rutile (both calcined at 350 °C).

For TiO_2 in the anatase form, the result of 100% color removal in 6000 seconds was obtained and subsequently kept constant up to 10,800 seconds, as shown in Figure 3(a). The reaction rate constant was 9.012×10^{-4}/s. The photocatalyst in the rutile form showed 98% color removal in 10,800 seconds of reaction (Figure 3(b)). However, the reaction rate constant was lower, with a value of 3.897×10^{-4}/s. Thus both forms (anatase and rutile) exhibited optimal removal of the coloration of the synthetic solution; however, even though both crystal structures are used as photocatalysts, the anatase form has a higher photocatalytic activity than the rutile for most reactions involving the degradation of organic contaminants (Luttrell *et al.* 2015).

This difference in behavior of the catalysts was influenced by the structural characteristics of each catalyst, such as the specific surface area (10 and 3 m^2/g for anatase and rutile, respectively), and band gap (3.12 for anatase and

3.19 eV for rutile). The evidence of color removal can be observed visually as indicated in the photograph inserted in Figure 3(a).

The sol-gel catalyst has specific characteristics determined by the methodology employed. The proposed methodology for the synthesis route of the sol-gel catalyst was promising with respect to TiO_2 modification for a band gap reduction (3.01 eV) and obtaining a high specific surface area (154 m^2/g), however in the catalytic tests, around 10,800 seconds, the percentage of color reduction of the methylene blue dye was only 5%. This is due to the fact that the structure is amorphous, being that the crystalline structure is one of the factors that has most influence in the photocatalytic performance of TiO_2 (Wang *et al.* 2016). The commercial catalyst did not exhibit color removal of the methylene blue in the established time of 10,800 seconds, not being effective in the degradation of the dye, and since the commercial TiO_2 semiconductor has a high band gap value ($E_{gap} \sim 3.19$ eV) it is excited only by UV light ($\lambda < 388.7$ nm) to inject electrons into the conduction band and leave gaps in the valence band. Consequently, the use of sunlight or visible light as a source of irradiation in the photocatalytic reaction with commercial TiO_2 is limited. A summary of the results obtained for the synthetic solution is presented in Table 6.

The result for the photolysis test with the synthetic methylene blue solution and the result of the adsorption test with the catalyst identified as the best of the catalysts studied, TiO_2 in anatase form, are shown in Figure 4.

The photolysis test, which causes the destruction of the organic molecules through the radiation, showed, at the end of the 10,800 seconds of reaction, a color removal around 35%. However, it should be noted that the degradation started only after about 5400 seconds. The adsorption result with the anatase TiO_2 catalyst indicated, at the beginning of the process, an inconstancy of the data, possibly a weak adsorption on the surface of the catalyst followed by a desorption. After approximately 3600 seconds of reaction, the stabilization of the adsorption process on the catalyst surface was constant, around 12%, until the end of the total time of 10,800 seconds. Thus, it is noticed that in both the photolysis and adsorption process, low degradation of methylene blue dye occurs, which demonstrates that the complete degradation of the dye takes place through the heterogeneous photocatalysis process.

Table 6 | Results of the photocatalytic tests for the methylene blue synthetic solution

Catalyst	Final concentration (kg/m³)	% of color removal in 10,800 s
TiO_2 commercial	0.02	*
TiO_2 sol-gel	0.019	5
TiO_2 rutile	0.0003	98
TiO_2 anatase	0	100

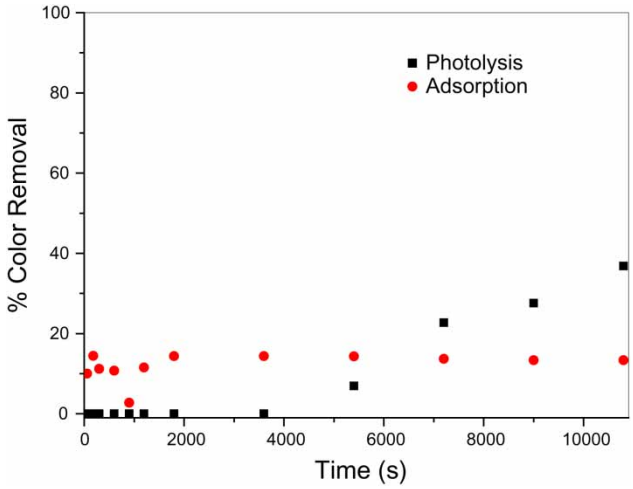

Figure 4 | Photolysis and adsorption test for the synthetic solution of methylene blue.

Sifted textile effluent

The photocatalytic tests performed with the sifted textile effluent sample were performed with the TiO_2 anatase photocatalyst due to its greater activity/efficiency in synthetic dye discoloration. The tests with the sifted textile effluent were conducted with different concentrations of TiO_2 anatase (2; 1 and 0.5 kg/m³) to verify the influence of the mass of the catalyst in the reaction. The results of degradation of the sieved textile effluent are shown in Figure 5.

It is observed that the highest percentage of color removal (71% in 10,800 s of reaction) was for the solution with a concentration of 1 kg/m³ of catalyst. The higher concentration of TiO_2 anatase (2 kg/m³) did not result in the higher efficiency, due to the effect of turbidity on the solution, which interferes with the penetration of light into the solution, presenting a decrease in the photocatalytic degradation process. On the other hand, the low catalyst concentration (0.5 kg/m³) limited the amount of active sites in the reaction. However, the kinetic curves for the three different concentrations are similar, as shown in Figure 5, which would justify a possible use of the TiO_2 anatase at the lowest studied concentration of 0.5 kg/m³.

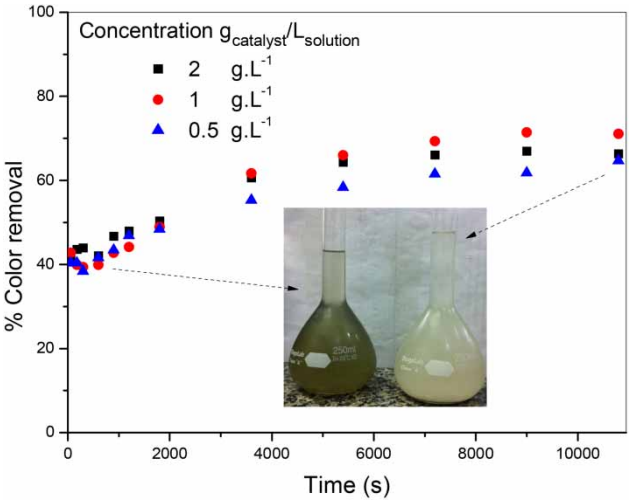

Figure 5 | Photocatalytic test with the sifted textile effluent at different concentrations of the TiO_2 catalyst in anatase form.

The color removal of the sifted textile effluent can be observed in detail in Figure 5. Where the flask on the left represents the effluent at the initial time of reaction (t = 0) and the flask on the right the same sample after 10,800 second of reaction using TIO_2 anatase 1 kg/m³. The photolysis and adsorption tests of the sifted textile effluent are presented in Figure 6. The photolysis test showed a color removal of 25%, while the adsorption test showed a 50% color removal, both at the end of 10,800 seconds. Despite the high percentage of color removal in the cited tests, it is not possible to state that all the removal was of the present dye, since it is possible to adsorb fibers with dye in the suspended particles, and they are sedimented after centrifugation.

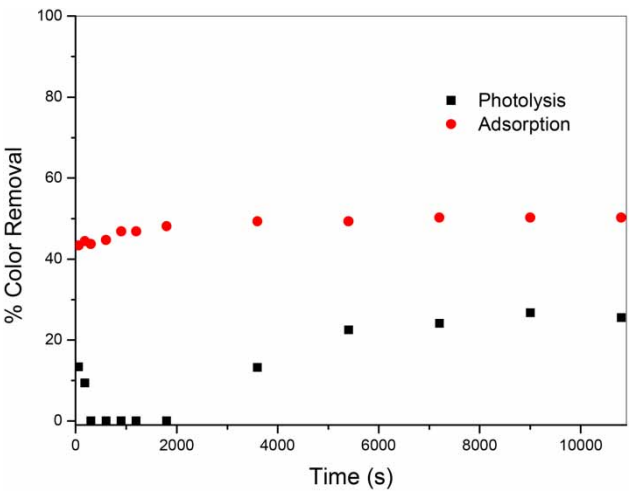

Figure 6 | Photolysis and adsorption test with sifted textile effluent and TiO_2 anatase.

Textile effluent untreated

The catalytic test for the untreated textile effluent sample was performed using the concentration of 1 kg/m³ of TiO_2 catalyst in anatase form. The amount of color removed per time is shown in Figure 7. In the photocatalytic test with the effluent untreated, a color removal of approximately 40% was obtained at the end of 10,800 seconds. This removal can be visually confirmed (detail of Figure 7) where the flask on the left shows the textile effluent untreated at the initial time reaction (t = 0) and the flask on the right represents the same sample after 10,800 seconds of photocatalytic reaction.

When comparing the color removal efficiency for the untreated and sifted effluent, it can be seen that the best result is for the sifted effluent, since the fibers and other solid components of the untreated effluent make it heterogeneous, forming a suspended layer that hinders the passage of radiation to the solution, as can be seen in the detail of Figure 7. As described in the literature (Touati *et al.* 2015) the treatment process of textile effluent with hydrogen peroxide and the 1% Ce-TiO_2 catalyst showed a color removal between 50% and 55% after 24 hours of artificial irradiation at an initial concentration of H_2O_2 of 10^{-1} M. Evidencing that the process shown in this present study, is efficient in the removal of color in a short period of time.

Many developing countries do not have adequate legislation (Standard Regulation) to color parameters such as Brazil, Cambodia and Thailand. However, other countries indicate that the parameter color should be not perceived after 1:20 dilution (discharge into surface

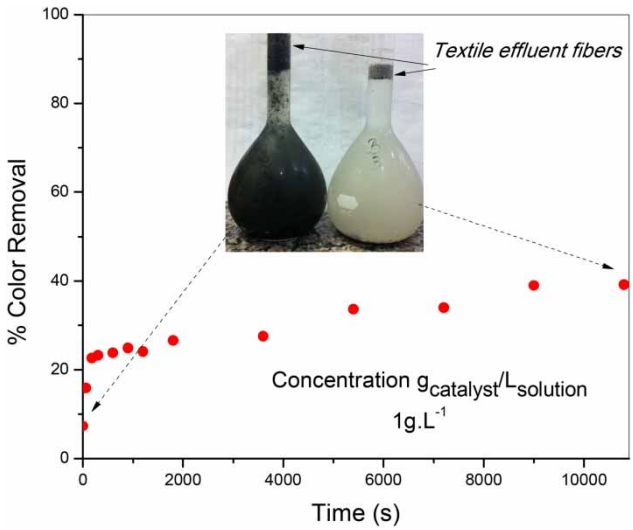

Figure 7 | Photocatalytic test with textile effluent untreated and TiO_2 anatase.

waters) and 1:40 (discharge into public sewer dilution) (ZDHC Programme 2015). Comparing the results obtained the synthetic effluent (see Figure 3, rutile and anatase catalyst at 10,800 s) could be directly discarded. On the other hand, for the sifted textile effluent and untreated textile effluent, despite the process efficiency, further dilution would be required.

COD, BOD and TDS analysis

The characterization of the untreated and sifted textile effluent before and after the treatments with the photocatalytic process is presented in Table 7. A considerable reduction in the analyzed parameters of total dissolved solids, chemical and BOD is observed, with the final COD values for both the sifted effluent and the raw effluent being within the current Brazilian legislation (<0.225 kg/m³) (Sanepar 2014). It was observed that there was a significant decrease in TDS, however, the values reached the minimum detection limit of the equipment used, being <0.005 kg/m³ for the effluent untreated and <0.0025 kg/m³ for the sifted effluent. The suspended solids limit for effluents from stabilization ponds is up to 0.15 kg/m³ in Europe and in the United States this value is around 0.08 kg/m³; for the BOD and COD parameters, the effluents should not exceed 0.025 and 0.125 kg/m³, respectively (Luttrell *et al.* 2015).

In general, the photocatalytic process with the TiO_2 in anatase form for the removal of color from the untreated and sifted effluents presented results that support the efficacy of the heterogeneous photocatalysis process in the treatment of textile effluent, removing its coloration and considerably reducing the parameters that are analyzed for disposal of the effluent into the environment.

Table 7 | Characterization of the untreated and sifted textile effluent before and after the photocatalytic reaction

		Textile effluent untreated	Sifted textile effluent
Before the photocatalytic reaction	TDS kg/m³	3.9833	0.9867
	COD kg/m³	7.2500	2.2333
	BOD kg/m³	0.9133	0.6900
After the photocatalytic reaction	TDS kg/m³	<0.0050	<0.0025
	COD kg/m³	0.1180	0.0064
	BOD kg/m³	0.1250	0.0358

CONCLUSIONS

The heterogeneous photocatalysis process proved to be very efficient in color removal of the methylene blue and textile effluent solutions, reducing COD, BOD and TDS concentrations significantly for the real effluent samples. The results of methylene blue dye discoloration were directly influenced by the structural differences (band gap, specific surface area and crystallinity) of the catalysts. It was observed that the crystallinity is a determining factor; this can be verified for the sol-gel catalyst as despite having presented a high surface area it has an amorphous structure and did not obtain significant results in the discoloration of methylene blue dye. The best result for the synthetic dye was obtained with the TiO_2 catalyst in the anatase phase, where 100% discoloration occurred in approximately 6000 seconds (band gap 3.12 eV, surface area 10 m^2/g). For the real effluent, comparing the efficiency between the tests carried out with sifted and untreated textile effluent, under the same conditions, it was noticed that for the sifted effluent the photocatalytic process had a higher discoloration result due to its greater homogeneity.

ACKNOWLEDGEMENT

The authors would like to thank Brazilian Agencies CAPES and CNPq for financial support of this study.

REFERENCES

Ahmad, A. A. & Hameed, B. H. 2009 Reduction of COD and color of dyeing effluent from a cotton textile mill by adsorption onto bamboo-based activated carbon. *Journal of Hazardous Materials* **172** (2–3), 1538–1543.

Cai, Y., Strømme, M. & Welch, K. 2013 Photocatalytic antibacterial effects are maintained on resin-based TiO_2 nanocomposites after cessation of UV irradiation. *PLoS ONE* **8** (10), e75929.

Carp, O., Huisman, C. L. & Reller, A. 2004 Photoinduced reactivity of titanium dioxide. *Progress in Solid State Chemistry* **32** (1–2), 33–177.

Dhanya, A. & Aparna, K. 2016 Synthesis and evaluation of TiO_2/Chitosan based hydrogel for the adsorptional photocatalytic degradation of azo and anthraquinone dye under UV light irradiation. *Procedia Technology* **24**, 611–618.

Fujishima, A., Rao, T. N. & Tryk, D. A. 2000 Titanium dioxide photocatalysis. *Journal of Photochemistry and Photobiology C: Photochemistry Reviews* **1** (1), 1–21.

Gupta, S. M. & Tripathi, M. 2011 A review of TiO_2 nanoparticles. *Chinese Science Bulletin* **56** (16), 1639–1657.

Han, F., Kambala, V. S. R., Srinivasan, M., Rajarathnam, D. & Naidu, R. 2009 Tailored titanium dioxide photocatalysts for the degradation of organic dyes in wastewater treatment: a review. *Applied Catalysis A: General* **359** (1–2), 25–40.

Hathaisamit, K., Sutha, W., Kamruang, P., Pudwat, S. & Teekasap, S. 2012 Decolorization of cationic yellow X-Gl 200% from textile dyes by TiO_2 films-coated rotor. *Procedia Engineering* **32**, 800–806.

Helali, S., Polo-López, M. I., Fernández-Ibáñez, P., Ohtani, B., Amano, F., Malato, S. & Guillard, C. 2013 Solar photocatalysis: a green technology for *E. coli* contaminated water disinfection. Effect of concentration and different types of suspended catalyst. *Journal of Photochemistry and Photobiology A: Chemistry* **276**, 31–40.

Landi, S., Carneiro, J., Ferdov, S., Fonseca, A. M., Neves, I. C., Ferreira, M., Parpot, P., Soares, O. S. G. P. & Pereira, M. F. R. 2017 Photocatalytic degradation of Rhodamine B dye by cotton textile coated with SiO_2-TiO_2 and SiO_2-TiO_2-HY composites. *Journal of Photochemistry and Photobiology A: Chemistry* **346**, 60–69.

Lenzi, G. G., Lenzi, M. K., Baesso, M. L., Bento, A. C., Jorge, L. M. M. & Santos, O. A. A. 2008 Cobalt, nickel and ruthenium-silica based materials synthesized by the sol–gel method. *Journal of Non-Crystalline Solids* **354** (42–44), 4811–4815.

Lenzi, G. G., Fávero, C. V. B., Colpini, L. M. S., Bernabe, H., Baesso, M. L., Specchia, S. & Santos, O. A. A. 2011 Photocatalytic reduction of Hg(II) on TiO_2 and Ag/TiO_2 prepared by the sol-gel and impregnation methods. *Desalination* **270** (1–3), 241–247.

Lenzi, G. G., Evangelista, R. F., Duarte, E. R., Colpini, L. M. S., Fornari, A. C., Menechini Neto, R., Jorge, L. M. M. & Santos, O. A. A. 2015 *Photocatalytic Degradation of Textile Reactive Dye Using Artificial Neural Network Modeling Approach*. Desalination and Water Treatment, pp. 1–13.

Luttrell, T., Halpegamage, S., Tao, J., Kramer, A., Sutter, E. & Batzill, M. 2015 Why is anatase a better photocatalyst than rutile? - Model studies on epitaxial TiO_2 films. *Scientific Reports* **4**, 1–8.

Miranda, A. C., Lepretti, M., Rizzo, L., Caputo, I., Vaiano, V., Sacco, O., Lopes, W. S. & Sannino, D. 2016 Surface water disinfection by chlorination and advanced oxidation processes: inactivation of an antibiotic resistant *E. coli* strain and cytotoxicity evaluation. *Science of the Total Environment* **554–555**, 1–6.

Oropeza, F. E., Harmer, J., Egdell, R. G. & Palgrave, R. G. 2010 A critical evaluation of the mode of incorporation of nitrogen in doped anatase photocatalysts. *Physical Chemistry Chemical Physics* **12**, 960–969.

Sales Solano, A. M., Costa de Araújo, C. K., Vieira de Melo, J., Peralta-Hernandez, J. M., Ribeiro da Silva, D. & Martínez-Huitle, C. A. 2013 Decontamination of real textile industrial effluent by strong oxidant species electrogenerated on diamond electrode: viability and disadvantages of this electrochemical technology. *Applied Catalysis B: Environmental* **130–131**, 112–120.

Sanepar 2014 Diretrizes para elaboração de estudos de disponibilidade hídrica e qualidade da água para projetos de SES (Guidelines for drafting water availability and water quality studies for SES projects), pp. 1–32. https://site.sanepar.com.br/sites/site.sanepar.com.br/files/informacoes-tecnicas/mps-manual-de-projetos-de-saneamento/Modulo_12_3_-_Diretrizes_Disponibilidade_Hidrica_-_SES.pdf (accessed 30 January 2018).

Souza, M. C. P., Lenzi, G. G., Colpini, L. M. S., Jorge, L. M. M. & Santos, O. A. A. 2011 Photocatalytic discoloration of reactive blue 5G dye in the presence of mixed oxides and with the addition of iron and silver. *Brazilian Journal of Chemical Engineering* **28** (3), 393–402.

Tokode, O., Prabhu, R., Lawton, L. A. & Robertson, P. K. J. 2017 A photocatalytic impeller reactor for gas phase heterogeneous photocatalysis. *Journal of Environmental Chemical Engineering* **5**, 3942–3948.

Touati, A., Hammedi, T., Najjar, W., Ksibi, Z. & Sayadi, S. 2015 Photocatalytic degradation of textile wastewater in presence of hydrogen peroxide: effect of cerium doping titania. *Journal of Industrial and Engineering Chemistry* **35**, 36–44.

Vamathevan, V., Tse, H., Amal, R., Low, G. & Mcevoy, S. 2001 Effects of Fe^{3+} and Ag^{+} ions on the photocatalytic degradation of sucrose in water. *Catalysis Today* **68**, 201–208.

Vohra, M. S. & Tanaka, K. 2003 Photocatalytic degradation of aqueous pollutants using silica-modified TiO_2. *Water Research* **37** (16), 3992–3996.

Wang, W. K., Chen, J. J., Zhang, X., Huang, Y. X., Li, W. W. & Yu, H. Q. 2016 Self-induced synthesis of phase-junction TiO_2 with a tailored rutile to anatase ratio below phase transition temperature. *Scientific Reports* **6**, 1–10.

Xiong, L., Sun, W., Yang, Y., Chen, C. & Ni, J. 2011 Heterogeneous photocatalysis of methylene blue over titanate nanotubes: effect of adsorption. *Journal of Colloid and Interface Science* **356**, 211–216.

ZDHC 2015 Textile Industry Wastewater Discharge Quality Standarts: Literature Review. Zero Discharge of Hazardous Chemicals Programme, pp. 1–84. http://www.roadmaptozero.com/fileadmin/pdf/WastewaterQualityGuidelineLitReview.pdf (accessed 27 April 2018).

First received 7 February 2018; accepted in revised form 30 May 2018. Available online 11 June 2018